Joint Graph-based User Scheduling and Beamforming in LEO-MIMO Satellite Communication Systems

Joint Graph-based User Scheduling and Beamforming in LEO-MIMO Satellite Communication Systems

Daniel Gaetano Riviello*, Bilal Ahmad*, Alessandro Guidotti†, Alessandro Vanelli-Coralli*
*Department of Electrical, Electronic, and Information Engineering (DEI),, University of Bologna, Bologna, Italy
†National Inter-University Consortium for Telecommunications (CNIT), Bologna, Italy
{daniel.riviello, bilal.ahmad6, a.guidotti, alessandro.vanelli}@unibo.it

***Abstract*—In this paper, a Low earth orbit (LEO) High-Throughput Satellite (HTS) Multi-User multiple-input multiple-output (MIMO) system is considered. With the objective of minimizing inter-beam interference among users, we propose a joint graph-based user scheduling and feed space beamforming framework for the downlink. First, we construct a graph where the vertices are the users and edges are based on a dissimilarity measure of their channels. Secondly, we design a low complexity greedy user clustering strategy, in which we iteratively search for the maximum clique in the graph. Finally, a Minimum Mean Square Error (MMSE) beamforming matrix is applied on a cluster basis with different power normalization schemes. A heuristic optimization of the graph density, i.e., optimal cluster size, is performed in order to maximize the system capacity. The proposed scheduling algorithm is compared with a position-based scheduler, in which a beam lattice is generated on ground and one user per beam is randomly selected to form a cluster. Results are presented in terms of achievable per-user capacity and show the superiority in performance of the proposed scheduler w.r.t. to the position-based approach.**

***Index Terms*—LEO, MU-MIMO, User Scheduling, Beamforming, MMSE**

I. Introduction

Satellite communication (Satcom) has gained a lot of popularity in the recent years, and they are expected to have a great impact on 5G and potentially the future 6G systems. With the inclusion of Non-Terrestrial Networks (NTN's) in 3GPPP Rel.17, the system flexibility, adaptability, and resilience and will be improved and the 5G coverage will be extended to rural and unserved areas. Low earth orbit (LEO) satellite communications have attracted a broad interest in the research community, as the much lower altitudes w.r.t. the geostationary earth orbit (GEO) could allow to provide global wireless access with enhanced data rates. Moreover, LEO satellite communication systems have much less stringent requirements on power consumption and transmission signal delays w.r.t. the GEO counterpart.

Massive multiple-input multiple-output (MIMO) has become an enabling technology for 5G terrestrial cellular wireless networks and is now expected to be integrated also in future satellite communication systems. Massive MIMO will increase available degrees of freedom, enhance spectral efficiency, and achieve high data rates [1]. A LEO satellite, equipped with antenna arrays with a large number of antenna elements, could serve many user terminals (UTs) in full frequency reuse schemes with the adoption of advanced digital beamforming techniques. The implementation of such techniques has been extensively addressed both for GEO and for LEO SatCom systems in [1]–[6]. The goal has been that of increasing the overall throughput in unicast or multicast systems, and addressing other major issues for SatCom-based beamforming, such as Channel State Information (CSI) retrieval and user scheduling or user grouping.

Since there are much more UTs on Earth than transmit antennas available on the satellite, user scheduling is necessary. Scheduling can be implemented by user selection or user grouping. While user selection algorithms search for only a single subset of all available users, in a user grouping algorithm all users are divided into groups which are then served in consecutive time slots. User grouping is an NP-complete problem and the solution to this problem is found in general via exhaustive search [7]. In [8] a sum rate maximization user grouping (SMUG) algorithm is proposed to divide users into several groups: users within the same group are simultaneously served by the satellite via space division multiple access (SDMA) and different groups of users are served in different time slots via time division multiple access (TDMA). In [9] the authors investigate into the design of user scheduling metrics for downlink Multi User MIMO (MU-MIMO) systems with heterogeneous users and propose two hybrid user scheduling algorithms that can capture fairness among users while maximizing sum rate capacity in a greedy manner, while in [10], a novel low complexity algorithm, named multiple antenna downlink orthogonal clustering (MADOC). The algorithm considers group number minimization and fairness among users and is an extension of the work in [9]. Finally, a graph-based user clustering strategy with two-stage beamforming for high-altitude platform (HAP) is proposed in [11]. The strategy is based on the construction of a graph by the similarity measure of correlation matrix distance, then user clustering is accomplished through the enumeration of all maximal cliques by exploiting the Bron-Kerbosch algorithm [12], which has combinatorial computational complexity.

In this paper, we propose a low-complexity graph-based approach for user scheduling for MU-MIMO LEO HTS and we show that the proposed algorithm can dramatically improve

the downlink sum capacity of the system. The clustering problem is modeled as an undirected and unweighted graph. Users constitute the vertices of the graph, and edges are based on a dissimilarity measure of their channels. The proposed greedy iterative procedure aims at minimizing the number of clusters by maximizing the size of each cluster and guaranteeing proportional fairness to all users. At each step, the maximum clique, i.e., the largest fully connected subgraph, is found through the efficient MaxCliqueDyn algorithm [13], the vertices belonging to the found maximum clique are assigned to a cluster, the graph is pruned by removing such vertices and the procedure stops when there are no more users left. For each cluster, SDMA is accomplished by means of MMSE beamforming. For the beamforming matrix, three different power normalizations are taken into account: Sum Power Constraint (SPC), Mean Power Constraint (MPC), and Per Antenna Power Constraint (PAC). Within the presented scenario, We also investigate for the optimal graph density, which maximizes the overall system capacity. The results are compared with a position-based scheduler, in which a beam lattice is generated on ground and one user per beam is randomly selected to form a cluster.

The rest of this paper is organized as: In Section II the system model is described, section III discusses the user scheduling based on maximum clique algorithm and graph theory, In section IV the numerical results and explanation is provided. Finally, Section V is the conclusion of the work.

Throughout this paper, and if not otherwise specified, the following notation is used: bold face lower case and bold face upper case characters denote vectors and matrices, respectively, $(\cdot)^\intercal$ denotes the matrix transposition operator, $(\cdot)^H$ denotes the matrix conjugate transposition operator, $[\mathbf{A}]_{i,j}$ denotes the entry in the i-th row and in the j-th column of matrix $\mathbf{A}$, $\mathrm{tr}(\mathbf{A})$ denotes the trace of matrix $\mathbf{A}$. The diag operator, when applied to a vector, i.e., $\mathbf{D} = \mathrm{diag}(\mathbf{a})$ constructs a diagonal matrix $\mathbf{D}$, whose main diagonal coincides with $\mathbf{a}$, otherwise, when the diag operator is applied to a matrix, i.e., $\mathbf{d} = \mathrm{diag}(\mathbf{A})$, extracts the main diagonal of matrix $\mathbf{A}$ into the column vector $\mathbf{d}$.

II. System Model

We consider a single multi-beam LEO satellite equipped with an on-board planar antenna array with N radiating elements, providing connectivity to K single-antenna uniformly distributed on-ground UTs by means of $S \leq N$ beams. We further assume that the LEO satellite always maintains a logical link with an on-ground gNB; to this aim, the satellite is assumed to be either directly connected to an on-ground gateway (GW) or to be connected through other LEO satellites in the constellation by means of Inter-Satellite Links (ISLs). The adopted system architecture is thoroughly described in [14]. The Radio Resource Management (RRM) scheduling (user grouping) and beamforming coefficients are computed at the on-ground gNB: different groups of users are served in different time slots via TDMA, while users within the same group are simultaneously served by the satellite via SDMA, i.e., the implementation of feed space digital beamforming techniques.

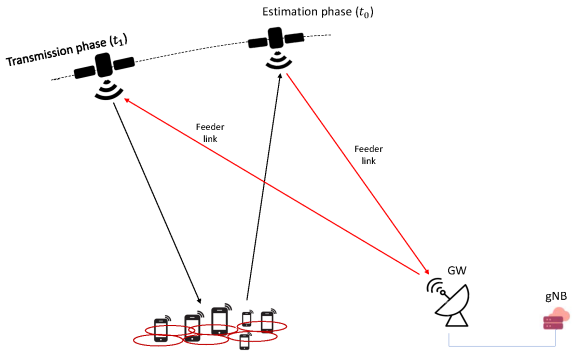

Fig. 1. System architecture with a single LEO satellite.

Both scheduling and beamforming require the estimation of the Channel State Information (CSI) provided by the UTs. As shown in Fig. 1, the CSI values are computed by the users at a time instant t_0; the scheduling and the beamforming matrices for every group of users are then computed at the gNB and, finally, actually used to transmit the beamformed symbols to the users at a time t_1. The latency $\Delta t = t_1 - t_0$ between the channel estimation phase and the transmission phase introduces a misalignment between the channel on which the scheduling and the beamforming matrices are computed and the actual channel through which the transmission occurs, which impacts the system performance. This latency can be computed as:

$$\Delta t = t_{ut,max} + 2t_{feeder} + t_p + t_{ad} \tag{1}$$

where: i) $t_{ut,max}$ is the maximum delay for the UTs requesting connectivity in the coverage area; ii) t_{feeder} is the delay on the feeder link, considered twice since the estimates are to be sent to the GW on the return link and then the beamformed symbols are sent on the forward link to the satellite; iii) t_p is the processing delay needed to compute the beamforming matrix; and iv) t_{ad} includes any additional delay.

The deployed antenna array model is based on ITU-R Recommendation M.2101 [15] illustrated in Fig. 2.

By default the antenna boresight directions is defined by the direction of the Sub Satellite Point (SSP). The point P is the position of the user terminal on the ground. The user directions are identified by (ϑ, φ) angles where the boresight direction is (0,0). We can now derive the direction cosines for the considered user as

$$u = \frac{P_y}{\|P\|} = \sin\vartheta \sin\varphi \tag{2}$$

$$v = \frac{P_z}{\|P\|} = \cos\vartheta \tag{3}$$

The total array response of the UPA in for the generic direction (ϑ_i, φ_i) can be expressed as a Kronecker product of the array responses of the 2 Uniform Linear Arrays (ULAs) lying on the y- and z-axis. We first define the $1 \times N_H$ Steering

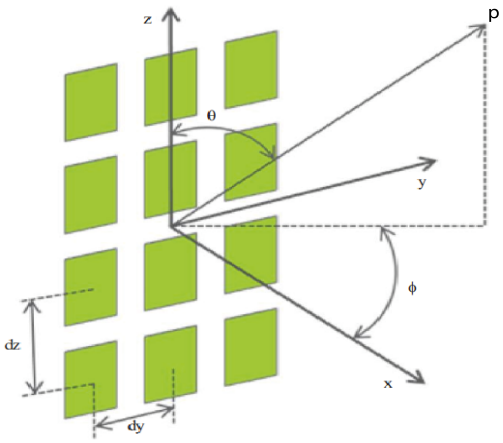

Fig. 2. Antenna Model Geometry from ITU-R M.2101-0 [15]

vector (SV) of the ULA along the y-axis $\mathbf{a}_H(\theta_i, \varphi_i)$ and the $1 \times N_V$ SV of the ULA along the z-axis $\mathbf{a}_V(\theta_i)$:

$$\mathbf{a}_H(\vartheta_i, \varphi_i) = \left[1, e^{jk_0 d_H \sin\vartheta_i \sin\varphi_i}, \ldots, e^{jk_0 d_H (N_H-1) \sin\vartheta_i \sin\varphi_i}\right] \tag{4}$$

$$\mathbf{a}_V(\vartheta_i) = \left[1, e^{jk_0 \cos\vartheta_i}, \ldots, e^{jk_0 d_V \pi (N_V-1) \cos\vartheta_i}\right]. \tag{5}$$

Where $k_0 = 2\pi\lambda$ is the wave number, N_H, N_V denotes the number of array elements on the horizontal (y-axis) and vertical (z-axis) directions with $N = N_H \cdot N_V$ and d_H, d_V denote the distance between adjacent array elements on the y- and z-axis respectively. We assume that the array is equipped with directive antenna elements, whose radiation pattern is denoted by $g_E(\vartheta_i, \varphi_i)$. Finally, we can express the $(1 \times N)$ SV of the UPA at the satellite targeted for the i-th user as the Kronecker product of the 2 SV's along each axis multiplied by the element radiation pattern:

$$\mathbf{a}(\vartheta_i, \varphi_i) = g_E(\vartheta_i, \varphi_i)\, \mathbf{a}_H(\vartheta_i, \varphi_i) \otimes \mathbf{a}_V(\vartheta_i) \tag{6}$$

The Channel State Information (CSI) vector at feed level $\mathbf{h}_i$ represents the channel between the N radiating elements and the generic i-th on-ground UT, with $i = 1, \ldots, K$, can be written as:

$$\mathbf{h}_i = G_i^{(rx)} \frac{\lambda}{4\pi d_i} \sqrt{\frac{L_i}{\kappa B T_i}} e^{-j\frac{2\pi}{\lambda} d_i} \mathbf{a}(\vartheta_i, \varphi_i) \tag{7}$$

in which, d_i is the slant range between the generic i-th user and the satellite, λ is the wavelength, $\kappa B T_i$ denotes the equivalent thermal noise power, with κ being the Boltzmann constant, B the user bandwidth (assumed to be the same for all users), and T_i the equivalent noise temperature of the i-th UT. L_i denotes all the additional losses per user, such as for example atmospheric, antenna, and cable losses. $G_i^{(rx)}$ denotes the receiving antenna gain for the i-th UT. The additional losses are computed as

$$L_i = L_{sha,i} + L_{atm,i} + L_{sci,i} \tag{8}$$

where $L_{sha,i}$ represents the log-normal shadow fading term, $L_{atm,i}$ the atmospheric loss, and $L_{sci,i}$ the scintillation, these terms are computed as per 3GPP TR 38.821 [16]

Collecting all of the K CSI vectors, it is possible to build a $K \times N$ complex channel matrix at system level $\mathbf{H} = [\mathbf{h}_1^\intercal, \mathbf{h}_2^\intercal, \ldots, \mathbf{h}_K^\intercal]^\intercal$, where the generic k-th row contains the CSI vector of the k-th user and the generic n-th column contains the channel coefficients from the n-th on-board feed towards the K on-ground users.

Given the set of all users to be scheduled, denoted with $\mathcal{U} = \{U_1, U_2, \ldots, U_K\}$, the Radio Resource Management (RRM) algorithm defines a possible users' partitioning $\{\mathcal{C}_1, \mathcal{C}_2, \ldots, \mathcal{C}_P\}$ where $\mathcal{C}_p \subseteq \mathcal{U}$ is defined as cluster and $|\mathcal{C}_p| = K_p$ is defined as the cardinality of the p-th cluster. Clusters are not necessarily disjoint sets of users, clearly $|\mathcal{C}_1 \cup \mathcal{C}_2 \cup \ldots \cup \mathcal{C}_P| = K$. We further assume that $T_{tot} = \sum_{p=1}^{P} |\mathcal{C}_p| \geq K$ time frames are available at the RRM, then for each time frame, the RRM selects the subset of users belonging to cluster $\mathcal{C}_p$ to be served, leading to a $K_p \times N$ complex scheduled channel matrix $\mathbf{H}_p = \mathcal{F}(\mathbf{H})$, where $\mathcal{F}(\cdot)$ denotes the RRM scheduling function, which is a sub-matrix of $\mathbf{H}$, i.e., $\mathbf{H}_p \subseteq \mathbf{H}$, which contains only the rows of the scheduled users in the p-th cluster. The selected beamforming algorithm computes for each cluster a $N \times K_p$ complex beamforming matrix $\mathbf{W}_p = [\mathbf{w}_1^{(p)}, \mathbf{w}_2^{(p)}, \ldots, \mathbf{w}_{K_p}^{(p)}]$, where $\mathbf{w}_i^{(p)}$ denotes the $N \times 1$ beamformer designed for the i-th user in the p-th cluster. The matrix $\mathbf{W}_p$ projects the K_p dimensional column vectors $\mathbf{s}_p = [s_1, s_2, \ldots, s_{K_p}]^\intercal$ containing the unit-variance user symbols onto the N-dimensional space defined by the antenna feeds. Thus, in the feed space, the computation of the beamforming matrix allows for the generation of a dedicated beam towards each user direction. The signal received by the i-th user in the p-th cluster can be expressed as follows:

$$y_k^{(p)} = \mathbf{h}_k \mathbf{w}_k^{(p)} s_k + \sum_{\substack{i=1 \\ i \neq k}}^{K_p} \mathbf{h}_k \mathbf{w}_i^{(p)} s_i + z_k^{(p)} \tag{9}$$

where $z_k^{(p)}$ is a circularly symmetric Gaussian random variable with zero mean and unit variance. The K_p-dimensional vector of received symbols in the p-th cluster is:

$$\mathbf{y}_p = \mathbf{H}_p^{(t_1)} \mathbf{W}_p^{(t_0)} \mathbf{s}_p + \mathbf{z}_p \tag{10}$$

It shall be noticed that, as previously discussed, the channel matrix $\mathbf{H}^{(t_0)}$ is used to compute the scheduling and the beamforming matrices $\mathbf{W}_p$ in the estimation phase at time instant t_0, while the beamformed symbols are sent to the users at a time instant t_1, in which the scheduled channel matrices are different and denoted as $\mathbf{H}_p^{(t_1)}$.

The Signal to interference plus noise ratio (SINR) for user k belonging to cluster p can be computed as

$$\mathrm{SINR}_k^{(p)} = \frac{\left\| \mathbf{h}_k \mathbf{w}_k^{(p)} \right\|^2}{1 + \sum_{\substack{i=1 \\ i \neq k}}^{K_p} \left\| \mathbf{h}_k \mathbf{w}_i^{(p)} \right\|^2} \tag{11}$$

In order to design a fair-proportional scheduler, given a total a total amount of T_{tot} time frames, each cluster is assigned

a number of time frames equal to the cardinality of the cluster K_p, therefore, the per-user achievable capacity can be computed as:

$$C_k = B \sum_{\substack{p \\ U_k \in \mathcal{C}_p}} \gamma_p \log_2 \left(1 + \text{SINR}_k^{(p)}\right) \tag{12}$$

where

$$\gamma_p = \frac{|\mathcal{C}_p|}{\sum_{p=1}^{P} |\mathcal{C}_p|} = \frac{K_p}{T_{tot}} \tag{13}$$

denotes the cluster weight.

The beamforming matrix $\mathbf{W}_p$, which is computed on a cluster basis, is based on the linear Minimum Mean Square Error (MMSE) equation:

$$\mathbf{W}_p = \left(\mathbf{H}_p^H \mathbf{H}_p + \alpha \mathbf{I}_N\right)^{-1} \mathbf{H}_p^H \tag{14}$$

where $\mathbf{I}_N$ indicates the $N \times N$ identity matrix and $\alpha = \frac{N}{P_t}$ is the regularisation factor with P_t the total on-board power. Finally, as detailed in [3], the power normalization is a fundamental step for beamforming so as to properly take into account the power that can be emitted both by the satellite and per antenna. We consider the following three options for power normalization:

1) The Sum Power Constraint (SPC): an upper bound is imposed on the total on-board power as:

$$\tilde{\mathbf{W}}_p = \frac{\sqrt{P_t}\mathbf{W}_p}{\sqrt{\text{tr}(\mathbf{W}_p \mathbf{W}_p^H)}} \tag{15}$$

SPC preserves the orthogonality of the beamformer columns but does not guarantee that the power transmitted from each feed will be upper bounded.

2) Per Antenna Constraint (PAC): the limitation is imposed per antenna with

$$\tilde{\mathbf{W}}_p = \sqrt{\frac{P_t}{N}} \left(\text{diag}\left(\text{diag}\left(\mathbf{W}_p \mathbf{W}_p^H\right)\right)\right)^{-\frac{1}{2}} \mathbf{W}_p \tag{16}$$

however the orthogonality in the beamformer columns here is disrupted.

3) Maximum Power Constraint (MPC) solution:

$$\tilde{\mathbf{W}}_p = \frac{\sqrt{P_t}\mathbf{W}_p}{\sqrt{N \max_j \left[\mathbf{W}_p \mathbf{W}_p^H\right]_{j,j}}} \tag{17}$$

the power per antenna is upper bounded and the orthogonality is preserved, but not the entire available on-board power is exploited.

III. Clique-based user scheduling

Let $\mathcal{G} = (\mathcal{V}, \mathcal{E})$ be an undirected and unweighted graph with vertex set $\mathcal{V}$ and edge set $\mathcal{E}$. A clique $\mathcal{Q}$ of $\mathcal{G}$ is a subset of the vertices, $\mathcal{Q} \subseteq \mathcal{V}$, such that every two distinct vertices are adjacent, i.e., $\mathcal{Q}$ is a complete subgraph. With reference to the LEO SatCom MIMO scenario, we construct a graph $\mathcal{G}$, whose set of vertices coincides with the set of users $\mathcal{U}$ and the edge set is constructed based a dissimilarity measure of their channels, i.e. the coefficient of correlation, which is defined as [17]

$$[\mathbf{\Psi}]_{i,j} = \frac{\left|\mathbf{h}_i \mathbf{h}_j^H\right|}{\|\mathbf{h}_i\| \, \|\mathbf{h}_j\|} \tag{18}$$

where $[\mathbf{\Psi}]_{i,j} \in [0, 1]$. The set of edges $\mathcal{E}$ of the $\mathcal{G}$ graph is completely determined by its adjacency matrix $\mathbf{A}$, whose entries are defined as:

$$[\mathbf{A}]_{i,j} = \begin{cases} 1, & [\mathbf{\Psi}]_{i,j} \leq \delta_{th} \\ 0, & [\mathbf{\Psi}]_{i,j} > \delta_{th} \end{cases} \tag{19}$$

where δ_{th} denotes a properly designed threshold. Equivalently, $\mathcal{E} = \{\{U_i, U_j\} \,|\, [\mathbf{A}]_{i,j} = 1\}$ where $\{U_i, U_j\}$ are unordered pairs of vertices. If an element of $\mathbf{A}$ is equal to 0, it means $\mathbf{h}_i$ and $\mathbf{h}_j$ are considered to be co-linear and there is no edge between U_i and U_j while if an element of $\mathbf{A}$ is equal to 1, it means that $\mathbf{h}_i$ and $\mathbf{h}_j$ are considered to be orthogonal, i.e., there is an edge between U_i and U_j and they can belong to the same cluster (or alternatively they can be co-scheduled). Based on these premises, a clique $\mathcal{Q}$ of the graph $\mathcal{G}$ represents a set of users with mutually uncorrelated channels, and therefore co-schedulable. Clearly, selecting the proper threshold δ_{th} plays a crucial role in the scheduler design as it determines the density of the graph $D(\mathcal{G})$, defined as the ratio of the number of edges $|\mathcal{E}|$ with respect to the maximum possible edge:

$$D(\mathcal{G}) = \frac{2|\mathcal{E}|}{|\mathcal{V}|\left(|\mathcal{V}| - 1\right)} \tag{20}$$

As stated in [7], the optimal value for δ_{th} depends on the channel characteristics and can only be heuristically determined, i.e., identified through simulations. The threshold determines an upper bound on the size of a clique and therefore the optimal number of users that can be efficiently multiplexed in the space domain by MMSE beamforming within a cluster.

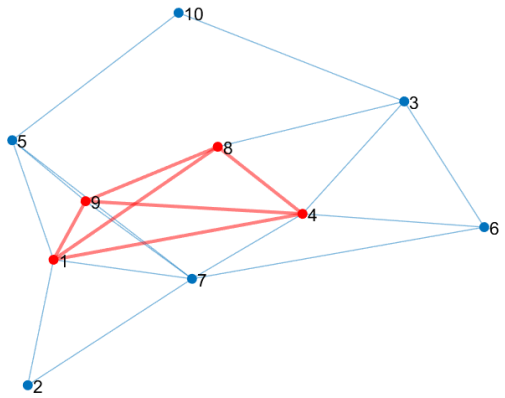

Fig. 3. Graph with $\mathcal{V} = \{U_1, \ldots, U_{10}\}$. Maximum clique $\mathcal{Q}_{\text{max}} = \{U_1, U_4, U_8, U_9\}$ shown in red.

Existing graph-based user clustering approaches are based on listing all maximal cliques, i.e., cliques that cannot be extended by including one more adjacent vertex. User clusters are then obtained by properly selecting a subset of the maximal

cliques [11]. Enumerating all maximal cliques has combinatorial complexity, and even with very efficient algorithms, such as the Bron-Kerbosch [12], the user clustering problem rapidly becomes intractable as the number of users increases.

We focus instead on a low-complexity approach based on maximum clique. A maximum clique $\mathcal{Q}_{\max} \subseteq \mathcal{V}$ is a clique, such that there is no clique with more vertices (as shown in Fig. 3). An efficient branch-and-bound algorithm for finding the maximum clique, termed MCQ, is presented in [18]. The algorithm is based on approximate graph coloring and appropriate sorting of the vertices and the coloring algorithm provides upper bounds to the size of the maximum clique. A more efficient maximum clique algorithm proposed by [13], called MaxCliqueDyn, uses improved coloring algorithm and extends the MCQ algorithm to include dynamically varying bounds.

The proposed user scheduling algorithm is a greedy iterative procedure that aims at minimizing the total number of P, given an optimized threshold δ_{th}. This is accomplished by:

1) maximizing the size of each cluster by iteratively finding the maximum clique of the updated graph;
2) creating disjoint sets of scheduled users, i.e., $\mathcal{C}_i \cap \mathcal{C}_j = \varnothing$, $\forall i, j$, which also minimizes T_{tot}, i.e., $T_{tot} = K$.

, As shown in Algorithm 1, the iterative procedure searches for the maximum clique $\mathcal{Q}_{\max}$ in the graph and declares it as a cluster; at each step the nodes in $\mathcal{Q}_{\max}$ and any edges connected to them are removed, the graph is updated after pruning. The procedure is repeated until there are no more vertices in the graph. Fairness is guaranteed among users by setting the cluster weight $\gamma_p = \frac{K_p}{K}$, i.e., the fraction of the overall resource assigned to $\mathcal{C}_p$, which could be a fraction of the total available bandwidth in FDMA, or a fraction of the total time slots in TDMA as described in Sec. II.

Algorithm 1 Iterative clique-based user scheduling algorithm

Input: Channel matrix $\mathbf{H}$, threshold δ_{th}
Output: Cluster sets $\mathcal{C}_p$ and cluster weights γ_p for $p = 1, \ldots, P$

Compute channel correlation distance matrix $\mathbf{\Psi}$ as in (18)
Compute adjacency matrix $\mathbf{A}$ as in (19)
Initialize remaining set of vertices with all users $\mathcal{R} = \mathcal{U}$
Create graph $\mathcal{G}(\mathcal{R}, \mathcal{E})$
Initialize $p = 1$
while $\mathcal{R} \neq \varnothing$ **do**
  $\mathcal{Q}_{\max} = \text{MaxCliqueDyn}(\mathcal{G})$
  $\mathcal{C}_p \leftarrow \mathcal{Q}_{\max}$
  $K_p \leftarrow |\mathcal{C}_p|$
  for all $U_i \in \mathcal{Q}_{\max}$ **do**
    for all $U_j \in \mathcal{R}$ **do**
      $\mathcal{E} = \mathcal{E} - \{U_i, U_j\}$
    end for
  end for
  $\mathcal{R} \leftarrow \mathcal{R} - \mathcal{Q}_{\max}$
  $p \leftarrow p + 1$
end while
$T_{tot} \leftarrow \sum_{p=1}^{P} K_p$
for p:=1 **to** P **do**
  $\gamma_p \leftarrow \frac{K_p}{T_{tot}}$
end for

IV. Simulation Setup and Results

TABLE I
Simulation Parameters.

Parameter	Value
Carrier frequency	2 GHz
System band	S (30 MHz)
Beamforming space	feed
Receiver type	VSAT
Receiver antenna gain	39.7 dBi
Noise figure	1.2 dB
Propagation scenario	Line of Sight
System scenario	urban
Total on-board power density, $P_{t,\text{dens}}$	4 dBW/MHz
Number of tiers	5
User density	0.05 user/km^2
Cluster size for position-based scheduler	91
Number of transmitters N	1024 (32×32 UPA)
Monte Carlo iterations	100

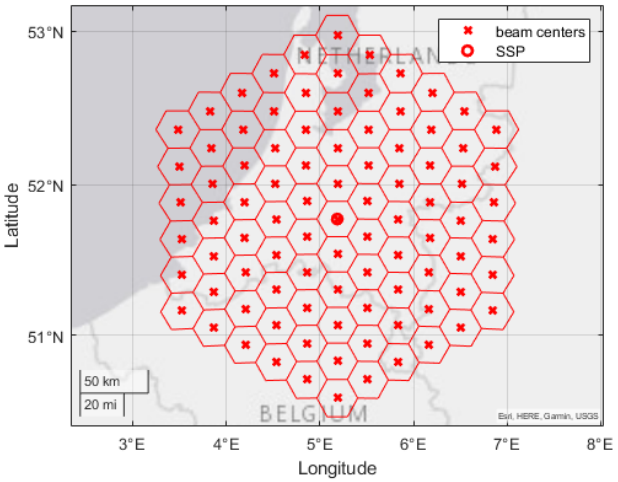

Fig. 4. Tier 5 beam lattice for position-based scheduler.

In this section, we present the outcomes of the extensive numerical simulations with the parameter setup provided in Tab. I. Please note that the assessment is performed in full buffer conditions, i.e., infinite traffic demand. We considered a single LEO HTS Satellite at a distance of 600 km from the earth. The users are uniformly distributed with the density of 0.05 users/Km^2, on average, the number of users $K = 2850$. The satellite is equipped with a UPA of 32×32 feeds. The user terminals are fixed and their receiver antenna gain $G_{\max}^{(rx)}$ is set to 39.7 dBi. The propagation scenario is the Line of Sight model based on TR 38.811 [19] and TR 38.821 [16]. In all tests, the performance of the clique-based scheduler is compared against a position-based scheduler, in which a beam lattice is generated on ground and one user per beam is randomly selected to form a cluster, as it is depicted in Fig. 4 for a tier 5 beam lattice consisting of 91 beams.

Within the presented scenario, we first performed a heuristic optimization (i.e., by extensive simulations) of the graph

TABLE II
SIMULATION RESULTS FOR THRESHOLD OPTIMIZATION

MMSE-	Capacity	Optimized δ_{th}	Average Cluster Size
SPC	7.71 Mbps	0.33	47.80
MPC	6.70 Mbps	0.25	42.02
PAC	3.84 Mbps	0.09	28.86

threshold value δ_{th} which maximizes the average per-user capacity. The graph threshold δ_{th} determines the density of the graph, and therefore the size of the maximum clique at each iteration, i.e., K_p. In particular, we aim at finding a trade-off between the minimization of the total time slots T_{tot} (maximization of the cluster size K_p), and the maximization of the average per-cluster SINR, $\frac{1}{K_p}\sum_{k=1}^{K_p}\text{SINR}_k^{(p)}$, which depends on the interference rejection capability of the per-cluster MMSE beamforming matrix $\mathbf{W}_p$, i.e., the ability to separate users only in the spatial domain. Clearly, this capability decreases as the number of users increases within a cluster. The results of the graph threshold optimization are show in Fig. 5 and 6. The average per-user capacity has been computed with a per-cluster MMSE beamforming matrix with SPC, MPC and PAC normalizations, respectively.

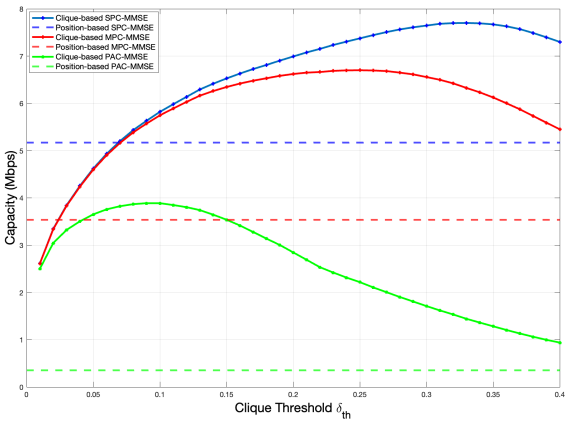

Fig. 5. Graph threshold δ_{th} optimization for average per-user capacity maximization.

Fig. 6 reports the mean cluster size as a function of the capacity. By recalling that in position-based scheduling the cluster size remains fixed, $K_p = 91, \forall p$, it can be noted that the clique-based scheduler produces clusters of smaller size, suggesting that interference management in a Tier 5 beam lattice becomes more problematic. With regards to the clique-based scheduler, SPC and MPC normalizations allow a larger cluster size w.r.t. PAC, which has a reduced interference rejection capability since it disrupts the MMSE solution. Tab. II summarizes the experimentally found graph threshold values and mean cluster sizes for each MMSE normalization. After graph threshold optimization, we show the Cumulative Distribution Function (CDF) of the user's capacity for both clique-based and position-based schedulers. Figs. 7 and 8

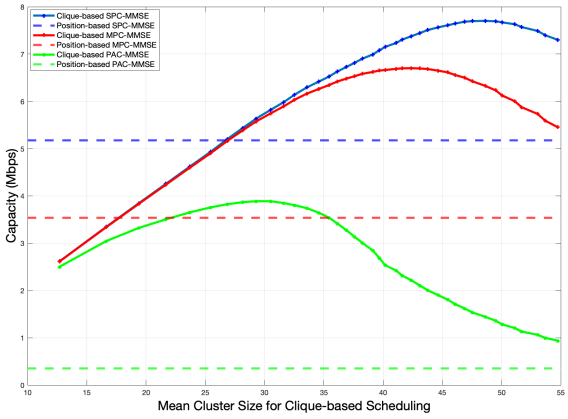

Fig. 6. Clique-based scheduler mean cluster size vs. average per-user capacity.

show the CDF of user's capacity and SINR, respectively, with an optimized MMSE-SPC graph threshold $\delta_{th} = 0.33$. The clique-based scheduler shows an improvement in terms of average per-user capacity of 4 Mbps and in terms of SINR of more than 20 dB with reference to MMSE-SPC normalization method. Figs. 9 and 10 show the CDF of users' capacity with an optimzed MMSE-MPC graph threshold $\delta_{th} = 0.25$ and MMSE-PAC $\delta_{th} = 0.09$ respectively. The gap in capacity between clique-based and position-based scheduler is evident in theses cases, too. Another important observation is that the clique-based scheduler also shows an improved fairness among users w.r.t the position-based one, i.e., the variance of the capacity is reduced (steeper CDF curve).

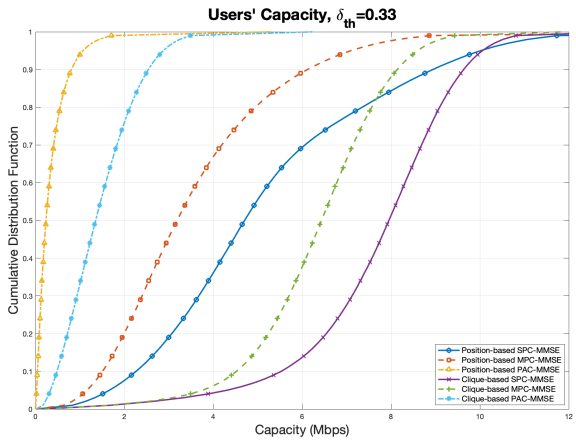

Fig. 7. CDF of users' capacity with graph threshold $\delta_{th} = 0.33$ optimized for MMSE-SPC.

V. CONCLUSION

In this work, we have proposed a greedy iterative user scheduling procedure based on the maximum clique algorithm and we have compared its performance against a position-based approach for a single LEO satellite MU-MIMO system.

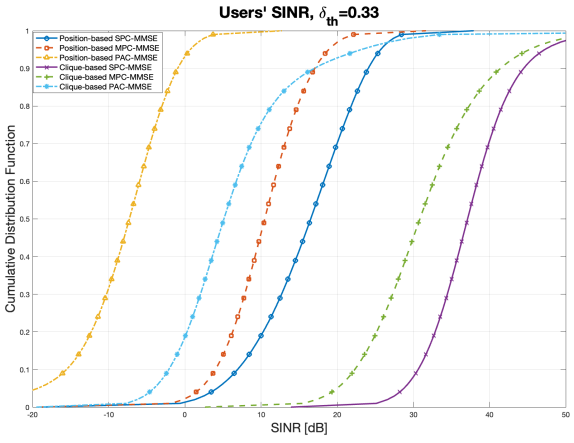

Fig. 8. CDF of users' SINR with graph threshold $\delta_{th} = 0.33$ optimized for MMSE-SPC.

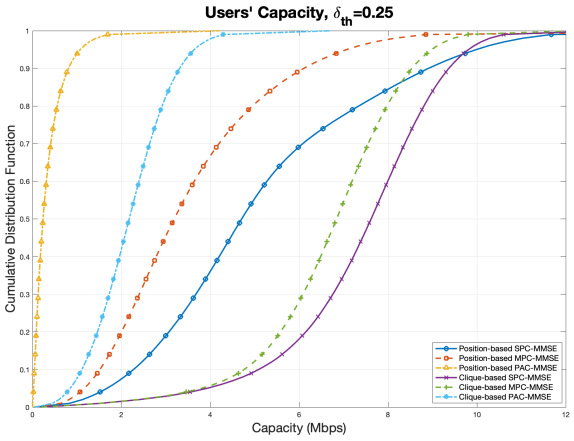

Fig. 9. CDF of users' capacity with graph threshold $\delta_{th} = 0.25$ optimized for MMSE-MPC.

For each time slot, a digital MMSE beamforming matrix allows to spatially separate the scheduled users and we considered three power normalizations for the beamforming matrix: SPC, MPC, and PAC. The results have been presented in terms of achievable per-user capacity and SINR and they show that the performance for clique based scheduling is highly improved as compared to the position based scheduling. Future works will improve the presented system model with the inclusion of multiple moving satellites. Furthermore, also non graph-based scheduling approaches will be taken into account as well as other digital beamforming methods.

VI. Acknowledgments

This work has been funded by the European Union Horizon-2020 Project DYNASAT (Dynamic Spectrum Sharing and Bandwidth-Efficient Techniques for High-Throughput MIMO Satellite Systems) under Grant Agreement 101004145. The views expressed are those of the authors and do not necessarily represent the project. The Commission is not liable for any use that may be made of any of the information contained therein.

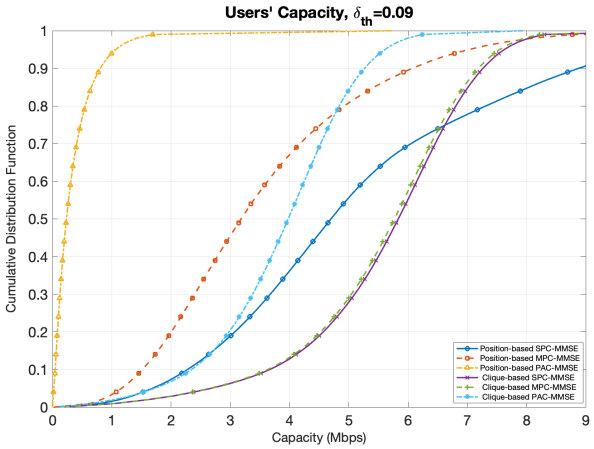

Fig. 10. CDF of users' capacity with graph threshold $\delta_{th} = 0.09$ optimized for MMSE-PAC.

References

[1] L. You, K. -X. Li, J. Wang, X. Gao, X. -G. Xia and B. Ottersten, "Massive MIMO Transmission for LEO Satellite Communications". in *IEEE Journal on Selected Areas in Communications*, vol. 38, no. 8, pp. 1851-1865, Aug. 2020, doi: 10.1109/JSAC.2020.3000803.

[2] P.-D. Arapoglou, K. Liolis, M. Bertinelli, A. Panagopoulos, P. Cottis, and R. De Gaudenzi, "Mimo over satellite: A review", *IEEE communications surveys & tutorials*, vol. 13, no. 1, pp. 27–51, 2010.

[3] A. Guidotti and A. Vanelli-Coralli, "Design Trade-Off Analysis of Precoding Multi-Beam Satellite Communication Systems", *2021 IEEE Aerospace Conference (50100)*, 2021, pp. 1-12, doi: 10.1109/AERO50100.2021.9438169.

[4] A. Guidotti and A. Vanelli-Coralli, "Clustering strategies for multicast precoding in multibeam satellite systems", *International Journal of Satellite Communications and Networking*, vol. 38, no. 2, pp. 85–104, 2020.

[5] A. Guidotti and A. Vanelli-Coralli, "Geographical Scheduling for Multicast Precoding in Multi-Beam Satellite Systems", *2018 9th Advanced Satellite Multimedia Systems Conference and the 15th Signal Processing for Space Communications Workshop (ASMS/SPSC)*, 2018, pp. 1-8, doi: 10.1109/ASMS-SPSC.2018.8510728.

[6] M. Á. Vázquez et al., "Precoding in Multibeam Satellite Communications: Present and Future Challenges", in *IEEE Wireless Communications*, vol. 23, no. 6, pp. 88-95, December 2016, doi: 10.1109/MWC.2016.1500047WC.

[7] E. Castaneda, A. Silva, A. Gameiro, and M. Kountouris, "An Overview on Resource Allocation Techniques for Multi-User MIMO Systems", *IEEE Communications Surveys & Tutorials*, vol. 20, no. c, pp. 1–1, 2016.

[8] H. Chen and C. Qi, "User Grouping for Sum-Rate Maximization in Multiuser Multibeam Satellite Communications", *ICC 2019 - 2019 IEEE International Conference on Communications (ICC)*, 2019, pp. 1-6, doi: 10.1109/ICC.2019.8761875.

[9] X. Yi and E. K. S. Au, "User Scheduling for Heterogeneous Multiuser MIMO Systems: A Subspace Viewpoint", in *IEEE Transactions on Vehicular Technology*, vol. 60, no. 8, pp. 4004-4013, Oct. 2011, doi: 10.1109/TVT.2011.2165976.

[10] K. Storek and A. Knopp, "Fair User Grouping for Multibeam Satellites with MU-MIMO Precoding", *GLOBECOM 2017 - 2017 IEEE Global Communications Conference*, 2017, pp. 1-7, doi: 10.1109/GLOCOM.2017.8255098.

[11] P. Ji, L. Jiang, C. He and D. He, "Graph Based User Clustering for HAP Massive MIMO Systems With Two-stage Beamforming", *2019 22nd International Symposium on Wireless Personal Multimedia Communications (WPMC)*, 2019, pp. 1-6, doi: 10.1109/WPMC48795.2019.9096130.

[12] C. Bron and J. Kerbosch, "Algorithm 457: finding all cliques of an undirected graph", *Communications of the ACM*, vol. 16, no. 9, pp: 575–577, Sep. 1973.

[13] J. Konc and D. Janezic, "An improved branch and bound algorithm for the maximum clique problem", *MATCH Commun. Math. Comput. Chem.*, 2007, 58, pp. 569-590.

[14] A. Guidotti, C. Amatetti, F. Arnal, B. Chamaillard and A. Vanelli-Coralli. "Location-assisted precoding in 5G LEO systems: architectures and performances", *2022 Joint European Conference on Networks and Communications & 6G Summit (EuCNC/6G Summit)*, 2022, arXiv:2204.02655 [cs.IT].

[15] ITU-R Radiocommunication Sector of ITU, "Modelling and simulation of IMT networks and systems for use in sharing and compatibility studies (M.2101-0)", Feb. 2017.

[16] 3GPP TR 38.821 V16.1.0, "Solutions for NR to support non-terrestrial networks (NTN) (Release 16)", May 2021.

[17] J. E. Gentle, *Matrix algebra: theory, computations, and applications in statistics*, Springer Science & Business Media, 2007.

[18] E. Tomita and T. Seki, "An Efficient Branch-and-Bound Algorithm for Finding a Maximum Clique", *Proceedings of the 4th International Conference on Discrete Mathematics and Theoretical Computer Science*, 2003, pp. 278-289, doi:10.5555/1783712.1783736.

[19] 3GPP TR 38.811 V15.4.0, "Study on New Radio (NR) to support non-terrestrial networks (Release 15)", Sep. 2020.